Available online at www.sciencedirect.com
SCIENCE DIRECT®
International Journal of Solids and Structures 42 (2005) 3533–3547
INTERNATIONAL JOURNAL OF SOLIDS and STRUCTURES
www.elsevier.com/locate/ijsolstr

Super element approach to cable passing through multiple pulleys

F. Ju *, Y.S. Choo *

Centre for Offshore Research and Engineering, Department of Civil Engineering, National University of Singapore, No. 1 Engineering Drive 2, Singapore 117576, Singapore

Received 25 March 2004; received in revised form 8 October 2004
Available online 18 November 2004

Abstract

A parametric super element model for cable passing through multiple pulleys is presented in this study for the static analysis of structures. The amounts of cable passages over pulleys are introduced as additional degrees-of-freedoms in the finite element model and the relationship between cable tensions at the two sides of each pulley is imposed based on the friction law or empirical data. The proposed finite element model is firstly verified by a simple pulley cable system and then applied to the analysis of real complex engineering structures. The verification results satisfy the static equilibrium and deformation compatibility conditions of the structural system and basic engineering principles. With the application of the proposed super element model, the global deformation and stress distribution for structures with multiple-pulley cable systems can be effectively and accurately computed. Numerical results for structural analysis show that the effect of friction of pulleys on the cable tensions is significant and the friction-free and fixed models both give unrealistic and incorrect results in cable tensions in some cases.

Keywords: Finite element; Cable; Pulley; Frictional effect; Structural analysis; Lifting

1. Introduction

Even the most complex and advanced structures are built out of certain simple structural components. One such component is the pulley cable system, which is widely used in cars, cranes, robots, fitness equipment, guyed and suspended structures. Structural simplicity, compactness, low friction and the abilities to absorb shock and transfer forces are some of the advantages for using cable pulley systems.

* Corresponding authors. Tel.: +65 6874 2667; fax: +65 6779 1635 (F. Ju), tel.: +65 6874 2994; fax: +65 6779 1635 (Y.S. Choo).
E-mail address: cvecys@nus.edu.sg (Y.S. Choo).

0020-7683/$ - see front matter © 2004 Elsevier Ltd. All rights reserved.
doi:10.1016/j.ijsolstr.2004.10.014

The ability of distributing and transferring load over a long distance through a complex geometric path is probably the most significant benefit for applying multiple-pulley cable systems. In this case, the net force is distributed across multiple cables or many loops of a continuous cable with multiple pulleys, and the tension in the each cable segment can thus be reduced. For this reason, multiple pulley-cable systems are used in the hoisting and luffing systems of cranes (Shapiro et al., 1991), where continuous cables, passing through or looping around many pulleys mounted on crane structures, link the payload and the boom structure to winches. This advantage is also applied at shipbuilding industry, as it will be discussed later in this paper, where spreader beams with cables passing through multiple pulleys are designed to spread forces to many lift points at ship structures.

Methods of static and dynamic analysis and the behavior of cables were thoroughly studied by Ozdemir (1979), Fried (1982), Leonard (1988), Gosling and Korban (2001). With respect to the modeling of cable passing through a pulley, Aufaure (1993, 2000) proposed finite element models to study the deformation of electric transmission lines/cables based on the assumption of the equal tensions in the cable segments at the two sides of a pulley. In real case, friction exists between bearings and the shaft and between the cable and the pulley surface (Ravikumar and Chattopadhyay, 1999 and Singru and Modak, 2001), resulting in different tensions at the two side of a pulley. Similar frictional effects on rigging slings in heavy lift system were also investigated by Choo et al. (1997), Lee et al. (2003) and Ju (1999).

In actual application, a cable may pass through multiple pulleys to transmit power and force from an engine or winch to other parts of the system, and the analysis of whole structural system should be integrated with an appropriate representation of such multiple-pulley cable system. If friction between pulleys and cable is negligible, the tensions at each segment of a cable should be the same, while the presence of friction consequently requires the cable tensions at two sides of a pulley to be at a certain ratio governed by the friction law. In this regard, the pulley cable system functions as both a structural component and a link constraint. The objective of this study is to develop an effective finite element scheme for the multiple-pulley cable system including the frictional effect which can be effectively integrated in the global structural analysis.

In this paper, a super element model including the frictional effect between cables and pulleys is presented for the static analysis of the global structural behaviour with multiple-pulley cable system. The amounts of cable passages (including slips) over pulleys are introduced as new unknowns in addition to the nodal translations in the element displacement vector. Each sub-element in the super-element model is essentially simplified as a linear tensile element, and the relationship between the forces in two adjacent sub-elements on the two sides of a pulley is then imposed based on the friction law or empirical data. The super element can be considered parametric in the sense that the number of pulleys linked to a continuous cable is a parameter in the formulations of element matrices and, once it is programmed in a software system, can be readily used as a normal element model without any difficulties. The advantage of parametric representation makes this super element model effective in computation and application.

Verification for the proposed finite element model is made by a simple pulley cable system, followed by the application and discussion of this finite element model in the numerical analysis of tower crane system and complex lifting system with pulley spreader beams. The verification results satisfy the static equilibrium and deformation compatibility conditions of the structural system and basic engineering principles. Numerical results for real applications show that the friction between the cable and pulleys has a significant effect on the cable tensions. The friction-free and fixed models both give unrealistic and incorrect results in cable tensions in some case. The proposed finite element model for the pulley cable system integrates tension ratios due to the frictional effects and deformation compatibility of the whole structural system into the computational process and, therefore, effective and accurate.

The basic assumption in this study lies on the fact that the axial load at the cable system is dominant in heavily loaded system, and each cable segment between two pulleys is straight and elastic. The bending or contact effect of cable over pulleys is neglected in this study to focus on the global effects of the pulley cable

system. For the analysis of the detailed interaction between a cable and a pulley, a global–local approach may be adopted, and the present model can provide the global response with enough accuracy for a detailed local analysis.

2. Finite element formulations

Fig. 1 shows a continuous cable passing through multiple intermediate pulleys, while the centres of these pulleys connect to other structural members and experience elastic deformations. It can be seen that the pulleys are $n-2$ in number. The whole system can be considered as a super element with n nodes and $n-1$ segments or sub-elements. The normal nodal displacements are indicated as δ_{xi}, δ_{yi}, δ_{zi} $(i=1,n)$ in the figure. The cable may pass from one side of a pulley to the other side due to the rotation of pulley, frictional slip of cable over pulley, or both of them. The amount of cable passed from one side is equal to that received at the other side and termed as cable passage around a pulley denoted as s_i $(i=2,n-1)$ as shown in Fig. 1. It can be seen that, if the two ends of the cable are connected to fully-constrained structure members or equipment without any rigid body movement or slip, the amount of cable passed at a pulley is actually a part of the elastic deformation of the whole cable. Physically, this kind of cable passage is a natural way in the system to mobilize the forces at the two sides of a pulley.

2.1. Sub-element analysis

The objective of the sub-element analysis in this section is to establish the relationship between nodal displacements and nodal forces of sub-element, which will be used later to form the stiffness matrix of the super element.

Fig. 2 shows a typical sub-element with the two end nodes i and $i+1$ located at (x_i, y_i, z_i) and $(x_{i+1}, y_{i+1}, z_{i+1})$, respectively. The subscripts in the figure denote for nodes while superscripts for sub-elements. For example, $f_{xi+1}^{(i)}$ represents the x component of the nodal force at node $i+1$ of the ith sub-element, while u_i simply the axial deformation at node i. This convention will be kept in this study.

To simplify the analysis, the dimension of the pulley is neglected in the element configuration but is considered in building up the relationship between the forces at the two sides of pulleys. Based on this simplification, the centres of the pulley are taken as the nodes for the super element, and deformations of the pulley centres are therefore the same as those at the node where two segments of cable are meet. The nodal displacements and forces in both local sub-element and global coordinate systems are shown in the figure.

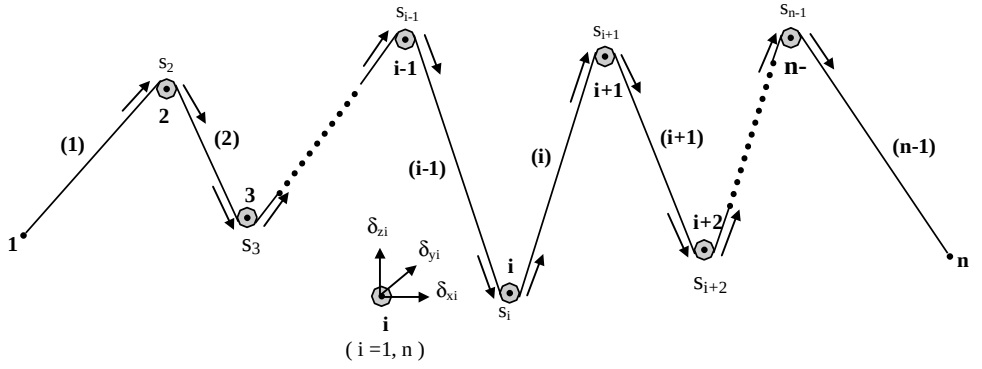

Fig. 1. A pulley-cable super element with n nodes.

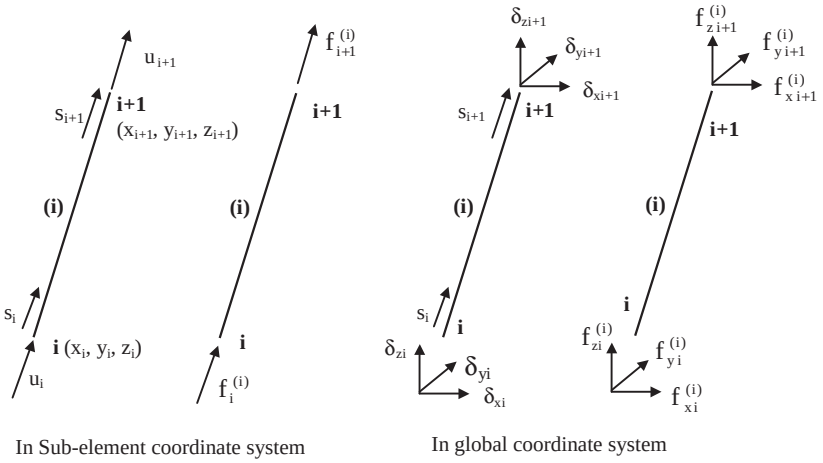

Fig. 2. Components of nodal displacements and forces in a typical sub-element.

Since the cable can only take axial tension, the relationship of nodal displacements and force can be established as:

$$\begin{Bmatrix} f_i^{(i)} \\ f_{i+1}^{(i)} \end{Bmatrix} = \begin{bmatrix} k^{(i)} & -k^{(i)} \\ -k^{(i)} & k^{(i)} \end{bmatrix} \begin{Bmatrix} u_i + s_i \\ u_{i+1} + s_{i+1} \end{Bmatrix} = k^{(i)} \begin{bmatrix} 1 & -1 & 1 & -1 \\ -1 & 1 & -1 & 1 \end{bmatrix} \begin{Bmatrix} u_i \\ u_{i+1} \\ s_i \\ s_{i+1} \end{Bmatrix} \tag{1a}$$

where $f_i^{(i)}$, u_i, s_i and $f_{i+1}^{(i)}$, u_{i+1}, s_{i+1} are the axial force, deformation and the cable passages at nodes i and $i+1$, respectively. The nominal stiffness of the sub-element $k^{(i)}$ is defined as:

$$k^{(i)} = \frac{E^{(i)} A^{(i)}}{L^{(i)}} \tag{1b}$$

where $E^{(i)}$, $A^{(i)}$ and $L^{(i)}$ are the Young's modulus, area of cross section and length of the sub-element.

Transforming nodal forces and displacements from local sub-element coordinates to global coordinates gives:

$$\begin{Bmatrix} f_i^{(i)} \\ f_{i+1}^{(i)} \end{Bmatrix} = \begin{bmatrix} \boldsymbol{\lambda}^{(i)} & 0 \\ 0 & \boldsymbol{\lambda}^{(i)} \end{bmatrix} \begin{Bmatrix} \mathbf{F}_i^{(i)} \\ \mathbf{F}_{i+1}^{(i)} \end{Bmatrix} \tag{2a}$$

and

$$\begin{Bmatrix} u_i \\ u_{i+1} \\ s_i \\ s_{i+1} \end{Bmatrix} = \begin{bmatrix} \boldsymbol{\lambda}^{(i)} & 0 & 0 & 0 \\ 0 & \boldsymbol{\lambda}^{(i)} & 0 & 0 \\ 0 & 0 & 1 & 0 \\ 0 & 0 & 0 & 1 \end{bmatrix} \begin{Bmatrix} \boldsymbol{\Delta}_i \\ \boldsymbol{\Delta}_{i+1} \\ s_i \\ s_{i+1} \end{Bmatrix} \tag{2b}$$

where $\{\mathbf{F}_i^{(i)}\}$, $\{\mathbf{F}_{i+1}^{(i)}\}$, $\{\boldsymbol{\Delta}_i\}$ and $\{\boldsymbol{\Delta}_{i+1}\}$ are the nodal force and displacement vectors at the global coordinate system as shown in Fig. 2 defined by

$$\{\mathbf{F}_i^{(i)}\} = \begin{bmatrix} f_{xi}^{(i)} & f_{yi}^{(i)} & f_{zi}^{(i)} \end{bmatrix}^{\mathrm{T}}, \quad \{\mathbf{F}_{i+1}^{(i)}\} = \begin{bmatrix} f_{xi+1}^{(i)} & f_{yi+1}^{(i)} & f_{zi+1}^{(i)} \end{bmatrix}^{\mathrm{T}} \tag{2c}$$

and

$$\{\mathbf{\Delta}_i\} = [\,\delta_{xi} \quad \delta_{yi} \quad \delta_{zi}\,]^{\mathrm{T}}, \quad \{\mathbf{\Delta}_{i+1}\} = [\,\delta_{xi+1} \quad \delta_{yi+1} \quad \delta_{zi+1}\,]^{\mathrm{T}}, \tag{2d}$$

with

$$[\boldsymbol{\lambda}^{(i)}] = \begin{bmatrix} \lambda_x^{(i)} & \lambda_y^{(i)} & \lambda_z^{(i)} \end{bmatrix} \tag{2e}$$

and the directional cosines of the sub-element given as:

$$\begin{aligned} \lambda_x^{(i)} &= \frac{x_{i+1} - x_i}{L^{(i)}} \\ \lambda_y^{(i)} &= \frac{y_{i+1} - y_i}{L^{(i)}} \\ \lambda_z^{(i)} &= \frac{z_{i+1} - z_i}{L^{(i)}} \end{aligned} \tag{2f}$$

By substituting Eqs. (2a) and (2b) into Eq. (1a) and using the orthogonal property of the transformation matrix, the following element matrix equation is obtained:

$$\begin{Bmatrix} \mathbf{F}_i^{(i)} \\ \mathbf{F}_{i+1}^{(i)} \end{Bmatrix}_{6\times 1} = \begin{bmatrix} \mathbf{k}_{\Delta\Delta}^{(i)} & -\mathbf{k}_{\Delta\Delta}^{(i)} & \mathbf{k}_{\Delta s}^{(i)} & -\mathbf{k}_{\Delta s}^{(i)} \\ -\mathbf{k}_{\Delta\Delta}^{(i)} & \mathbf{k}_{\Delta\Delta}^{(i)} & -\mathbf{k}_{\Delta s}^{(i)} & \mathbf{k}_{\Delta s}^{(i)} \end{bmatrix}_{6\times 8} \begin{Bmatrix} \mathbf{\Delta}_i \\ \mathbf{\Delta}_{i+1} \\ s_i \\ s_{i+1} \end{Bmatrix}_{8\times 1} \tag{3a}$$

where

$$[\mathbf{k}_{\Delta\Delta}^{(i)}]_{3\times 3} = k^{(i)}[\boldsymbol{\lambda}^{(i)}]^{\mathrm{T}}[\boldsymbol{\lambda}^{(i)}] \tag{3b}$$

and

$$\{\mathbf{k}_{\Delta s}^{(i)}\}_{3\times 1} = k^{(i)}[\boldsymbol{\lambda}^{(i)}]^{\mathrm{T}} \tag{3c}$$

Considering the force equilibrium conditions at each nodes, following equation for the super element can be obtained:

$$\{\mathbf{F}\}_{3n\times 1} = [\,\mathbf{K}_{\Delta\Delta} \quad \mathbf{K}_{\Delta s}\,]_{3n\times(4n-2)} \begin{Bmatrix} \mathbf{\Delta} \\ \mathbf{S} \end{Bmatrix}_{(4n-2)\times 1}, \tag{4}$$

where $\{\mathbf{F}\}_{3n\times 1}$ and $\{\mathbf{\Delta}\}_{3n\times 1}$ are the conventional nodal forces and displacements of the super element, $[\mathbf{K}_{\Delta\Delta}]_{3n\times 3n}$ and $[\mathbf{K}_{\Delta s}]_{3n\times n}$, which are respectively assembled from Eqs. (3b) and (3c), are:

$$[\mathbf{K}_{\Delta\Delta}] = \begin{bmatrix} \mathbf{k}_{\Delta\Delta}^{(1)} & -\mathbf{k}_{\Delta\Delta}^{(1)} & & & & & \\ -\mathbf{k}_{\Delta\Delta}^{(1)} & \mathbf{k}_{\Delta\Delta}^{(1)} + \mathbf{k}_{\Delta\Delta}^{(2)} & \cdots & & \mathbf{0} & & \\ & -\mathbf{k}_{\Delta\Delta}^{(2)} & \cdots & -\mathbf{k}_{\Delta\Delta}^{(i-1)} & & & \\ & & \cdots & \mathbf{k}_{\Delta\Delta}^{(i-1)} + \mathbf{k}_{\Delta\Delta}^{(i)} & \cdots & & \\ & & & -\mathbf{k}_{\Delta\Delta}^{(i)} & \cdots & -\mathbf{k}_{\Delta\Delta}^{(n-1)} & \\ & \mathbf{0} & & & \cdots & \mathbf{k}_{\Delta\Delta}^{(n-1)} + \mathbf{k}_{\Delta\Delta}^{(n)} & -\mathbf{k}_{\Delta\Delta}^{(n)} \\ & & & & & -\mathbf{k}_{\Delta\Delta}^{(n)} & \mathbf{k}_{\Delta\Delta}^{(n)} \end{bmatrix}_{3n\times 3n} \tag{4a}$$

$$[\mathbf{K}_{\Delta s}] = \begin{bmatrix} -\mathbf{k}_{\Delta s}^{(1)} & & & & & & \\ \mathbf{k}_{\Delta s}^{(1)} + \mathbf{k}_{\Delta s}^{(2)} & -\mathbf{k}_{\Delta s}^{(2)} & & & & \mathbf{0} & \\ -\mathbf{k}_{\Delta s}^{(2)} & \mathbf{k}_{\Delta s}^{(2)} + \mathbf{k}_{\Delta s}^{(3)} & \cdots & -\mathbf{k}_{\Delta s}^{(i-1)} & & & \\ & -\mathbf{k}_{\Delta s}^{(3)} & \cdots & \mathbf{k}_{\Delta s}^{(i-1)} + \mathbf{k}_{\Delta s}^{(i)} & \cdots & -\mathbf{k}_{\Delta s}^{(n-2)} & \\ & & \cdots & -\mathbf{k}_{\Delta s}^{(i)} & \cdots & \mathbf{k}_{\Delta s}^{(n-2)} + \mathbf{k}_{\Delta s}^{(n-1)} & -\mathbf{k}_{\Delta s}^{(n-1)} \\ & \mathbf{0} & & & \cdots & -\mathbf{k}_{\Delta s}^{(n-1)} & \mathbf{k}_{\Delta s}^{(n-1)} + \mathbf{k}_{\Delta s}^{(n)} \\ & & & & & & -\mathbf{k}_{\Delta s}^{(n)} \end{bmatrix}_{3n\times(n-2)} \tag{4b}$$

and $\{\mathbf{S}\}_{n\times 1}$ is the vector of cable passages at all the nodes defined by

$$\{\mathbf{S}\}_{(n-2)\times 1} = [\, s_2 \quad s_3 \quad \cdots \quad s_{n-2} \quad s_{n-1} \,]^{\mathrm{T}} \tag{4c}$$

It can be seen from Eq. (4) that, due to the presence of cable passages, n more equations are needed to make the relationship between nodal forces and displacements complete. These additional equations can be established by considering the force relationship between the forces in the cable at the two sides of a pulley.

2.2. Relationship of tensions at two sides of a pulley

Fig. 3 shows the tensions in the cable around a pulley with or without slip between the drum and cable. Neglecting the inertia effect of the pulley, the relationship between the tensions at the two sides on verge of slipping or slipping is given by Euler's equation as

$$T_2 = \alpha T_1 \tag{5a}$$

with the tension ratio α given as

$$\alpha = \mathrm{e}^{\mu\theta} \tag{5b}$$

where μ is the coefficient of friction and θ is the contact angle as indicated in Fig. 3. Detailed derivation of the above equations can be found in Beer and Johnston (1996). This tension ratio α can also be obtained empirically and referred as "loss coefficient" by Shapiro et al. (1991).

Eq. (5a) will be applied to build the relationship between forces in the two adjacent sub-elements.

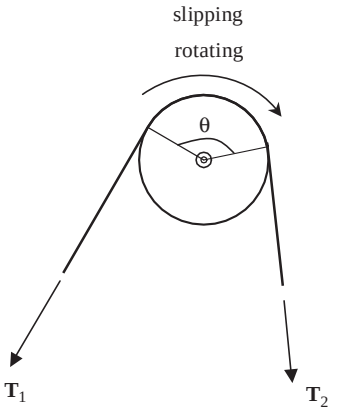

Fig. 3. Cable passing through a pulley.

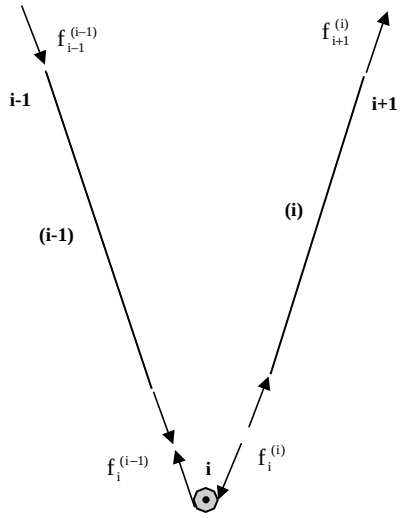

Fig. 4. Forces relationship of two sub-elements around a pulley.

Considering the forces at node i where sub-elements $i-1$ and i are connected to the ith pulley as shown in Fig. 4. Substituting Eq. (2b) into Eq. (1a), the nodal axial forces can be expressed as:

$$\begin{Bmatrix} f_i^{(i)} \\ f_{i+1}^{(i)} \end{Bmatrix} = k^{(i)} \begin{bmatrix} \boldsymbol{\lambda}^{(i)} & -\boldsymbol{\lambda}^{(i)} & 1 & -1 \\ -\boldsymbol{\lambda}^{(i)} & \boldsymbol{\lambda}^{(i)} & -1 & 1 \end{bmatrix} \begin{Bmatrix} \boldsymbol{\Delta}_i \\ \boldsymbol{\Delta}_{i+1} \\ s_i \\ s_{i+1} \end{Bmatrix} \tag{6a}$$

Similarly, for sub-element $(i-1)$, the same relationship is

$$\begin{Bmatrix} f_{i-1}^{(i-1)} \\ f_i^{(i-1)} \end{Bmatrix} = k^{(i-1)} \begin{bmatrix} \boldsymbol{\lambda}^{(i-1)} & -\boldsymbol{\lambda}^{(i-1)} & 1 & -1 \\ -\boldsymbol{\lambda}^{(i-1)} & \boldsymbol{\lambda}^{(i-1)} & -1 & 1 \end{bmatrix} \begin{Bmatrix} \boldsymbol{\Delta}_{i-1} \\ \boldsymbol{\Delta}_i \\ s_{i-1} \\ s_i \end{Bmatrix} \tag{6b}$$

Based on Eq. (5a), the relationship between the axial forces in the two sub-elements at node i can be expressed as:

$$f_i^{(i)} = -\alpha_i f_i^{(i-1)} \tag{7a}$$

where the negative sign results from the convention of force in the sub-element and α_i is dependent on the coefficient of friction and contact angle at the pulley defined by Eq. (5b).

Substituting $f_i^{(i)}$ and $f_i^{(i-1)}$ from Eqs. (6a) and (6b) into Eq. (7a) gives:

$$\begin{aligned} 0 = & \left[-\alpha_i k^{(i-1)} \boldsymbol{\lambda}^{(i-1)} \quad \alpha_i k^{(i-1)} \boldsymbol{\lambda}^{(i-1)} + k^{(i)} \boldsymbol{\lambda}^{(i)} \quad -k^{(i)} \boldsymbol{\lambda}^{(i)} \quad -\alpha_i k^{(i-1)} \quad \alpha_i k^{(i-1)} + k^{(i)} \quad -k^{(i)} \right] \\ & \times \left[\boldsymbol{\Delta}_{i-1} \quad \boldsymbol{\Delta}_i \quad \boldsymbol{\Delta}_{i+1} \quad s_{i-1} \quad s_i \quad s_{i+1} \right]^{\mathrm{T}} \end{aligned} \tag{7b}$$

or

$$\begin{aligned} 0 = & \left[-\alpha_i \mathbf{k}_{s\Delta}^{(i-1)} \quad \alpha_i \mathbf{k}_{s\Delta}^{(i-1)} + \mathbf{k}_{s\Delta}^{(i)} \quad -\mathbf{k}_{s\Delta}^{(i)} \quad -\alpha_i k^{(i-1)} \quad \alpha_i k^{(i-1)} + k^{(i)} \quad -k^{(i)} \right] \\ & \times \left[\boldsymbol{\Delta}_{i-1} \quad \boldsymbol{\Delta}_i \quad \boldsymbol{\Delta}_{i+1} \quad s_{i-1} \quad s_i \quad s_{i+1} \right]^{\mathrm{T}} \end{aligned} \tag{7c}$$

with

$$[\mathbf{k}_{s\Delta}^{(i)}] = k^{(i)}[\boldsymbol{\lambda}^{(i)}] \tag{7d}$$

Summating Eq. (7c) for $i = 2$ to $n-1$ gives:

$$\{\mathbf{0}\}_{(n-2)\times 1} = [\,\mathbf{K}_{s\Delta} \quad \mathbf{K}_{ss}\,]_{(n-2)\times(4n-2)} \begin{Bmatrix} \boldsymbol{\Delta} \\ \mathbf{S} \end{Bmatrix}_{(4n-2)\times 1} \tag{8}$$

where

$$[\mathbf{K}_{s\Delta}] = \begin{bmatrix} -\alpha_2\mathbf{k}_{s\Delta}^{(1)} & \alpha_2\mathbf{k}_{s\Delta}^{(1)}+\mathbf{k}_{s\Delta}^{(2)} & -\mathbf{k}_{s\Delta}^{(2)} & & & & & & \\ & -\alpha_3\mathbf{k}_{s\Delta}^{(2)} & \alpha_3\mathbf{k}_{s\Delta}^{(2)}+\mathbf{k}_{s\Delta}^{(3)} & -\mathbf{k}_{s\Delta}^{(3)} & & & & \mathbf{0} & \\ & & \cdots & \cdots & \cdots & & & & \\ & & & -\alpha_i\mathbf{k}_{s\Delta}^{(i-1)} & \alpha_i\mathbf{k}_{s\Delta}^{(i-1)}+\mathbf{k}_{s\Delta}^{(i)} & -\mathbf{k}_{s\Delta}^{(i)} & & & \\ & & & & \cdots & \cdots & \cdots & & \\ & \mathbf{0} & & & & -\alpha_{n-2}\mathbf{k}_{s\Delta}^{(n-3)} & \alpha_{n-2}\mathbf{k}_{s\Delta}^{(n-3)}+\mathbf{k}_{s\Delta}^{(n-2)} & -\mathbf{k}_{s\Delta}^{(n-2)} & \\ & & & & & & -\alpha_{n-1}\mathbf{k}_{s\Delta}^{(n-2)} & \alpha_{n-1}\mathbf{k}_{s\Delta}^{(n-2)}+\mathbf{k}_{s\Delta}^{(n-1)} & -\mathbf{k}_{s\Delta}^{(n-1)} \end{bmatrix}_{(n-2)\times 3n} \tag{8a}$$

and

$$[\mathbf{K}_{ss}] = \begin{bmatrix} \alpha_2 k^{(1)}+k^{(2)} & -k^{(2)} & & & & & & & \\ -\alpha_3 k^{(2)} & \alpha_3 k^{(2)}+k^{(3)} & -k^{(3)} & & & & & \mathbf{0} & \\ & \cdots & \cdots & \cdots & & & & & \\ & & -\alpha_i k^{(i-1)} & \alpha_i k^{(i-1)}+k^{(i)} & -k^{(i)} & & & & \\ & & & \cdots & \cdots & \cdots & & & \\ & \mathbf{0} & & & -\alpha_{n-2}k^{(n-3)} & \alpha_{n-2}k^{(n-3)}+k^{(n-2)} & -k^{(n-2)} & & \\ & & & & & -\alpha_{n-1}k^{(n-2)} & \alpha_{n-1}k^{(n-2)}+k^{(n-1)} & & \end{bmatrix}_{(n-2)\times(n-2)} \tag{8b}$$

2.3. Super element formulations

Summarizing Eqs. (8) and (4) gives the final relationship of between the general nodal displacements and forces:

$$\begin{Bmatrix} \mathbf{F} \\ \mathbf{0} \end{Bmatrix}_{(4n-2)\times 1} = [\mathbf{K}]_{(4n-2)\times(4n-2)} \begin{Bmatrix} \boldsymbol{\Delta} \\ \mathbf{S} \end{Bmatrix}_{(4n-2)\times 1} \tag{9}$$

where the stiffness matrix of the super element is

$$[\mathbf{K}] = \begin{bmatrix} \mathbf{K}_{\Delta\Delta} & \mathbf{K}_{\Delta s} \\ \mathbf{K}_{s\Delta} & \mathbf{K}_{ss} \end{bmatrix} \tag{9a}$$

with $[\mathbf{K}_{\Delta\Delta}]$, $[\mathbf{K}_{\Delta s}]$, $[\mathbf{K}_{s\Delta}]$ and $[\mathbf{K}_{ss}]$ given Eqs. (4a), (4b), (8a) and (8b), respectively.

It can be seen from Eqs. (8a) and (4b) that, with the presence of friction between the cable and pulley, the stiffness matrix $[\mathbf{K}]$ is generally unsymmetrical. This matrix will become symmetrical if the frictional effect is negligible since $[\mathbf{K}_{\Delta s}] = [\mathbf{K}_{s\Delta}]^{\mathrm{T}}$ when $\alpha = 1$.

3. Verifications and applications

In this section, one simple example of a cable passing through multiple pulleys is firstly discussed to verify the proposed super-element model, followed by two real examples to illustrate the application of this model in structural analysis. The diameter and Young's modulus of the cables are assumed to be 26 mm and 50 kN/mm^2, respectively.

3.1. A continuous cable passing through fixed pulleys

Static analysis of a continuous cable passing two pulleys, as shown in Fig. 5, is used to verify the proposed super element formulations, where one end of the cable may be considered to be connected to a winch with a pulling force of p and the other end to a structure member or a payload. It can be seen that this super element consists of four nodes and three sub-elements with two passage degrees-of-freedom denoted respectively as s_2 and s_3. The force and displacement boundary conditions are also indicated in the figure.

Applying Eq. (9) to this case, following relationship between nodal forces and displacements can be established:

$$\begin{Bmatrix} f_{1x} \\ f_{1y} \\ f_{2x} \\ f_{2y} \\ f_{3x} \\ f_{3y} \\ f_{4x} \\ f_{4y} \\ 0 \\ 0 \end{Bmatrix} = \begin{bmatrix} 0 & 0 & 0 & 0 & 0 & 0 & 0 & 0 & 0 & 0 \\ 0 & k^{(1)} & 0 & -k^{(1)} & 0 & 0 & 0 & 0 & -k^{(1)} & 0 \\ 0 & 0 & 0 & 0 & 0 & 0 & 0 & 0 & 0 & 0 \\ 0 & -k^{(1)} & 0 & k^{(1)}+k^{(2)} & 0 & -k^{(2)} & 0 & 0 & k^{(1)}-k^{(2)} & k^{(2)} \\ 0 & 0 & 0 & 0 & k^{(3)} & 0 & -k^{(3)} & 0 & 0 & k^{(3)} \\ 0 & 0 & 0 & -k^{(2)} & 0 & k^{(2)} & 0 & 0 & k^{(2)} & -k^{(2)} \\ 0 & 0 & 0 & 0 & -k^{(3)} & 0 & k^{(3)} & 0 & 0 & -k^{(3)} \\ 0 & 0 & 0 & 0 & 0 & 0 & 0 & 0 & 0 & 0 \\ 0 & -\alpha_2 k^{(1)} & 0 & \alpha_2 k^{(1)}-k^{(2)} & 0 & k^{(2)} & 0 & 0 & \alpha_2 k^{(1)}+k^{(2)} & -k^{(2)} \\ 0 & 0 & 0 & \alpha_3 k^{(2)} & k^{(3)} & -\alpha_3 k^{(2)} & -k^{(3)} & 0 & -\alpha_3 k^{(2)} & \alpha_3 k^{(2)}+k^{(3)} \end{bmatrix} \cdot \begin{Bmatrix} \delta_{1x} \\ \delta_{1y} \\ \delta_{2x} \\ \delta_{2y} \\ \delta_{3x} \\ \delta_{3y} \\ \delta_{4x} \\ \delta_{4y} \\ s_2 \\ s_3 \end{Bmatrix} \tag{10a}$$

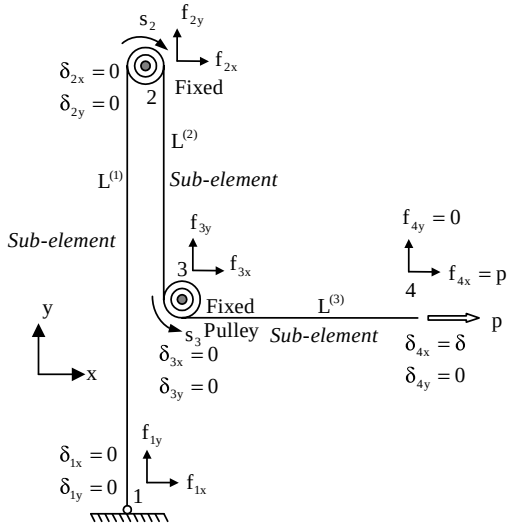

Fig. 5. A continuous cable passing through two fixed pulleys.

where α_2 and α_3 are the tension ratio at the two pulleys as indicated in Eqs. (5a) and (7a) and $k^{(i)}$ is the nominal stiffness of the sub-element defined by

$$k^{(i)} = EA/L^{(i)} \tag{10b}$$

with E, A and $L^{(i)}$ $(i = 1,2,3)$ being the Young's modulus, area of cross section and the lengths of the sub-elements, respectively.

Substituting force and displacement boundary conditions into Eq. (10a) yields:

$$\begin{Bmatrix} p \\ 0 \\ 0 \end{Bmatrix} = \begin{bmatrix} k^{(3)} & 0 & -k^{(3)} \\ 0 & \alpha_2 k^{(1)} + k^{(2)} & -k^{(2)} \\ -k^{(3)} & -\alpha_3 k^{(2)} & \alpha_3 k^{(2)} + k^{(3)} \end{bmatrix} \cdot \begin{Bmatrix} \delta \\ s_2 \\ s_3 \end{Bmatrix} \tag{10c}$$

Solving above equation gives the following results for displacement and cable passages:

$$\begin{cases} s_2 = \dfrac{p}{\alpha_2 \alpha_3 k^{(1)}} \\ s_3 = \dfrac{p}{\alpha_2 \alpha_3 k^{(1)}} + \dfrac{p}{\alpha_3 k^{(2)}} \\ \delta = \dfrac{p}{\alpha_2 \alpha_3 k^{(1)}} + \dfrac{p}{\alpha_3 k^{(2)}} + \dfrac{p}{k^{(3)}} \end{cases} \tag{10d}$$

Furthermore, nodal forces can be obtained from Eq. (10a) as

$$\begin{cases} f_{1x} = 0; \quad f_{1y} = \dfrac{-p}{\alpha_2 \alpha_3} \\ f_{2x} = 0; \quad f_{2y} = \dfrac{p}{\alpha_2 \alpha_3} + \dfrac{p}{\alpha_3} \\ f_{3x} = -p; \quad f_{3y} = \dfrac{-p}{\alpha_3} \end{cases} \tag{10e}$$

The results show that the tension at sub-element 2 reduces to p/α_3 due to the friction loss at lower pulley and tension at sub-element 3 further reduces to $p/\alpha_2\alpha_3$ because of frictional effect at upper pulley. The cable passage at upper pulley, s_2, equals to the elongation of sub-element 1, and that at lower pulley, s_3, equals to the elongation of sub-elements 2 and 3. The displacement at node 1, δ, is the axial displacement of the whole cable. If the friction at pulleys is small enough to be neglected, the tension ratios will be 1, resulting in equal tensions at all sub-elements. It can be seen that these results satisfy the static equilibrium and deformation compatibility conditions and engineering principles and, therefore, valid.

3.2. Structural analysis of tower crane including multiple-pulley cable systems

The quasistatic behaviour of a luffing tower crane is analyzed in this section to illustrate the application of the proposed element model for multiple-pulley cable system. Fig. 6a schematically shows the critical members and dimensions of the tower crane. It can be seen that the hoisting cable connects a load to a winch at location D through pulleys B and C, and the luffing cable connects jib structure, passing through the pulley J, to a winch at location K. As shown in Fig. 6b, most of the structural members are modeled as space frame elements and the counter weights and payload are modeled as lump mass. Two multiple-pulley cable elements proposed in this study are use to model the hoisting and luffing cables. Assuming the payload is being lifted up at a uniform speed, or it is intended to be lifted up with just enough tension from the winch to overcome the gravity and friction, the relationship among the tensions of the segments of the hoisting cable may be simply assumed as:

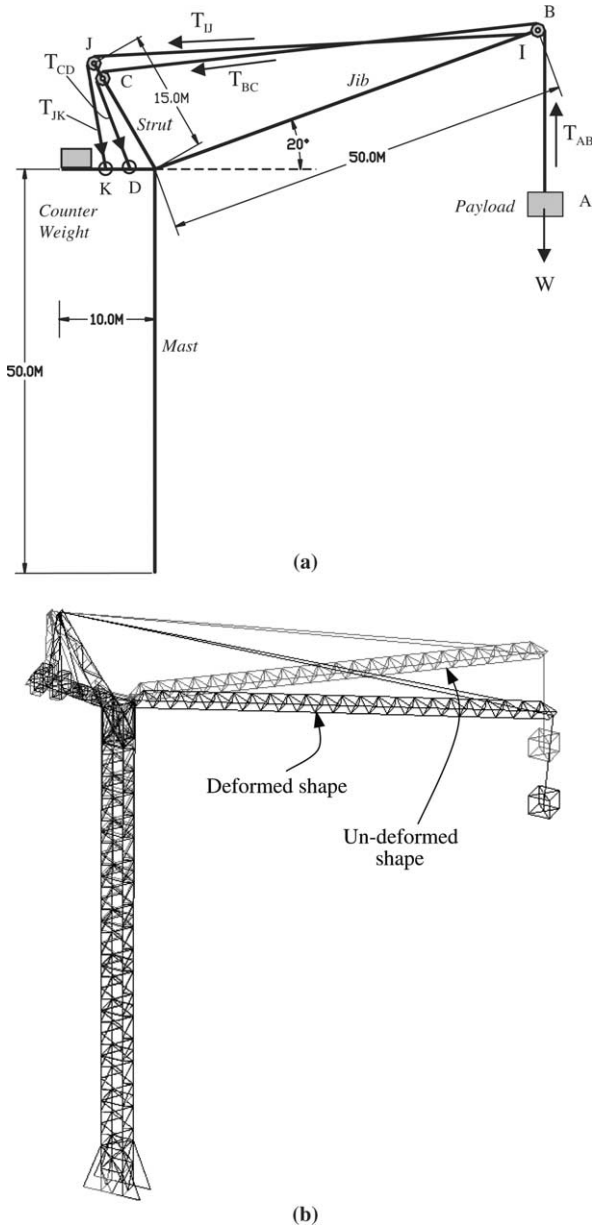

Fig. 6. (a) Schematic illustration of Tower Crane with pulley-cable system and (b) finite element model of tower crane with deformed and mesh.

$$\frac{T_{\mathrm{BC}}}{T_{\mathrm{AB}}} = \alpha_1$$
$$\frac{T_{\mathrm{CD}}}{T_{\mathrm{BC}}} = \frac{T_{\mathrm{JK}}}{T_{\mathrm{IJ}}} = \alpha_2 \tag{11}$$

Table 1
Cable tensions of tower crane in quasistatic analysis[a]

Assumption on tension ratio	Hoisting cable			Luffing cable	
	T_{AB} (W)	T_{BC} (W)	T_{CD} (W)	T_{IJ} (W)	T_{JK} (W)
$\alpha_1 = 1.00$; $\alpha_2 = 1.00$ (friction-free)	1.00	1.00	1.00	2.27	2.27
$\alpha_1 = 1.20$; $\alpha_2 = 1.05$	1.00	1.20	1.26	2.39	2.51
Fixed cable	1.00	2.64	3.60	1.01	3.04

[a] W is the weight of the payload.

Table 1 gives the tension at each segment of the hoisting and luffing cables in this quasistatic analysis with various assumptions on the tension ratio. For the friction-free assumption with $\alpha_1 = \alpha_2 = 1.0$, tension at each segment of the cable is equal. If each segment of the cables is assumed as fixed members, which can be modeled as linear truss or beam elements, the axial tensions of these segments will be purely determined by the global equilibrium condition and deformation compatibility of the structure without any imposed relationships among these forces. These are two extreme cases of the real structural behaviour.

In real case, the presence of friction at pulleys results in unequal tensions at the two adjacent segments of the cables as shown in the table with the corresponding deformed shape of the full model showing in Fig. 6b. A bigger tension ratio adopted at pulley B is due to the fact that hoisting cable normally goes many rounds around the pulley array at the tip of the jib (Shapiro et al., 1991) and even a slight friction accumulatively induces a significant effect on cable tensions. For instance, if the hoist cable goes five rounds around pulley B and the coefficient of friction is as small as 0.006, the tension ratio can be as large as 1.20 based on Euler's equation (from Eq. (5b), $\alpha = e^{0.006\times5\times2\pi} \approx 1.21$). It can be seen from the table that the effect of friction of pulleys on the cable tensions is significant and the friction-free and fixed models both give unrealistic and incorrect results in cable tensions. One can easily understand that incorrect prediction of cable tensions implies incorrect computational results of stresses and stiffness at some parts of the tower crane system. The strength of the proposed super element model for the pulley cable system is at the incorporation of tension ratios due to frictional effects and deformation compatibility of the whole structural system in an integrated computation. Therefore, the proposed numerical model gives realistic and correct results.

3.3. Structural analysis of rigging system with pulley spreader beams

Spreader beams with multiple pulleys are used in shipbuilding and the fabrication of large marine structures. Fig. 7 shows a typical rigging system with two pulley spreader beams and 24 lift points at the top of the deck structure. With the spreader beams in lift rigging system, compressive forces at module decks are minimized and the concentrating force at a particular location of the structure is comparative small due to the adoption of multiple lift points.

In the finite element analysis of this rigging system, the proposed super element model is used to model the multiple-pulley cable systems at the spreader beam. As it is shown in the figure, one super element consists of one continuous cable, 13 nodes and 5 fixed and 6 moveable pulleys, and therefore, 11 more degrees-of-freedom of cable passages over pulleys are introduced as indicated in Eqs. (4) and (4c). The total degrees-of-freedom of this super element will be 50 with 39 translations and 11 cable passages over pulley.

Table 2 gives the tensions at different segment of the cable at the two sides of pulleys. It can be seen from the table that, if the pulleys are well lubricated with negligible frictional loss ($\alpha = 1.0$), the tensions at all segment of the cable are the same and the resulting forces at lift points, passing through slings with tensions T_i ($i = 1, 6$), are almost uniformly distributed. This is the expected outcome of using pulley spreader beams. The global structural deformation for the case of friction-free is shown in the Fig. 7. However, the cumulative effect of friction at pulleys on force distribution can be significant as indicated in Table 2 with a tension ratio

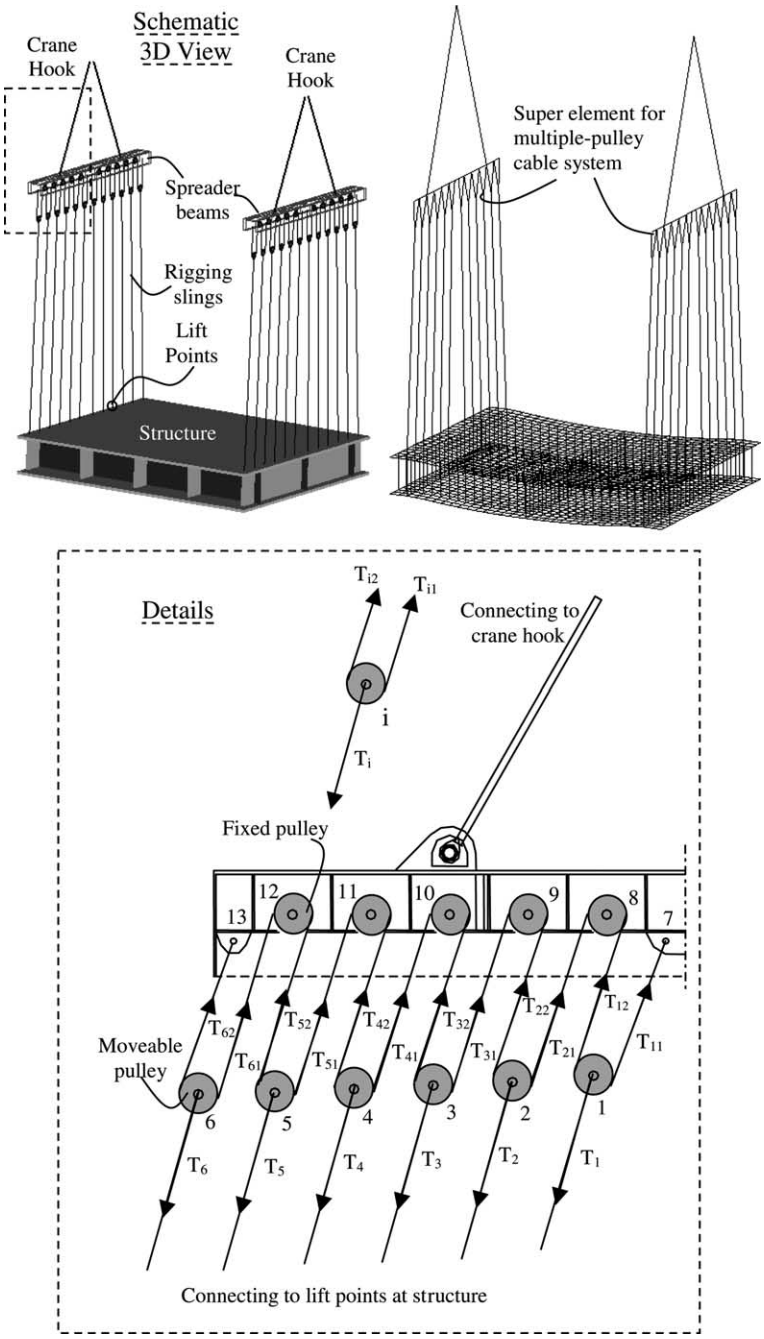

Fig. 7. Finite element modelling of lift system with pulley spreader beams.

of 1.05. In this case, the coefficient of friction at pulleys is assumed to be 0.015, the tension ratio α is thus 1.05 ($\alpha = e^{0.015\times\pi} \approx 1.05$) according to Eq. (5b), and the difference between the force at inner lift point, which is $T_1 = 0.212 \times (W/4)$, and that of outer lift point, which is $T_6 = 0.130 \times (W/4)$, can be as large as 39%.

Table 2
Cable tensions at pulley spreader rigging system[a]

	T_1		T_2		T_3		T_4		T_5		T_6	
	T_{11}	T_{12}	T_{21}	T_{22}	T_{31}	T_{32}	T_{41}	T_{42}	T_{51}	T_{52}	T_{61}	T_{62}
$\alpha = 1.00$	0.168		0.166		0.166		0.166		0.166		0.168	
	0.086	0.086	0.086	0.086	0.086	0.086	0.086	0.086	0.086	0.086	0.086	0.086
$\alpha = 1.05$	0.212		0.189		0.172		0.156		0.141		0.130	
	0.110	0.105	0.100	0.096	0.091	0.087	0.083	0.079	0.075	0.071	0.068	0.065

[a] $T_i \sim T_i \times (W/4)$, $T_{ij} \sim T_{ij} \times (W/4)$; W is the weight of the structure being lifted.

From the point of view of mechanics, the pulley spreader system can be considered as enforced constraint of forces at structures being lifted, and the structural deformation and stress distribution are totally different from those with conventional simply supported, fixed or even spring constraints. With the application of the proposed super element model, the global deformation and stress distribution for structures with multiple-pulley cable system can be effectively and accurately computed.

4. Conclusions

A parametric super element model for cable passing through multiple pulleys is proposed in this study for numerical analysis of structures. The amounts of cable passages over pulleys are introduced as additional degrees-of-freedoms in the finite element model. The relationship between cable tensions at the two sides of a pulley is imposed based on the friction law or empirical coefficient. The proposed model is firstly verified by a simple cable system with three fixed pulleys and then applied to two real engineering systems: tower crane system and lifting system with pulley spreader beams. The verification results satisfy the static equilibrium and deformation compatibility conditions of the structural system and basic engineering principles.

Numerical results for real applications show that the effect of friction of pulleys on the cable tensions is significant and the friction-free and fixed models both give unrealistic and incorrect results in cable tensions in some cases. The pulley spreader system can be considered as enforced constraints of forces at structures being lifted, and the structural deformation and stress distribution are totally different from those with conventional simply supported, fixed or spring constraints. The advantage of the proposed super element model for the pulley cable system is at the incorporation of tension ratios due to frictional effects and deformation compatibility of the whole structural system in an integrated computation. The global deformation and stress distribution of whole structural system can be effectively and accurately predicted.

References

Aufaure, M., 1993. A finite element of cable passing through a pulley. Computers and Structures 46 (5), 807–812.

Aufaure, M., 2000. Three-node cable element ensuring the continuity of the horizontal tension: a clamp-cable element. Computers and Structures 74 (2), 243–251.

Beer, F.B., Johnston, E.R., 1996. Vector Mechanics for Engineers: Statics. McGraw-Hill, New York.

Choo, Y.S., Ju, F., Lee, K.H., 1997. Static sling tensions in heavy lifts with doubled sling arrangement. International Journal of Offshore and Polar Engineering 7 (4), 313–322.

Fried, I., 1982. Large deformation static and dynamic finite element analysis of extensible cables. Computers and Structures 15 (3), 315–319.

Gosling, P.D., Korban, E.A., 2001. A bendable finite element for the analysis of flexible cable structures. Finite Elements in Analysis and Design 38 (2), 45–63.

Ju, F., 1999. Marine/offshore heavy lift system analysis and knowledge-based system development. Ph.D. thesis, National University of Singapore.

Lee, K.H., Choo, Y.S., Ju, F., 2003. Finite element modelling of frictional slip in heavy lift sling systems. Computers and Structures 81 (30), 2673–2690.

Leonard, J.W., 1988. Tension Structures. McGraw-Hill, New York.

Ozdemir, H., 1979. A finite element approach for cable problems. International Journal of Solids Structures 15 (6), 427–437.

Ravikumar, M., Chattopadhyay, A., 1999. Integral analysis of conveyor pulley using finite element method. Computers and Structures 71 (3), 303–332.

Shapiro, H.I., Shapiro, J.P., Shapiro, L.K., 1991. Cranes and Derricks. McGraw-Hill, New York.

Singru, P.M., Modak, J.P., 2001. Computer simulation of the dynamic and vibration response of a belt drive pulley. Journal of Sound and Vibration 242 (2), 277–293.